

Provided for non-commercial research and education use.
Not for reproduction, distribution or commercial use.



This article appeared in a journal published by Elsevier. The attached copy is furnished to the author for internal non-commercial research and education use, including for instruction at the authors institution and sharing with colleagues.

Other uses, including reproduction and distribution, or selling or licensing copies, or posting to personal, institutional or third party websites are prohibited.

In most cases authors are permitted to post their version of the article (e.g. in Word or Tex form) to their personal website or institutional repository. Authors requiring further information regarding Elsevier's archiving and manuscript policies are encouraged to visit:

<http://www.elsevier.com/copyright>



Contents lists available at ScienceDirect

Talanta

journal homepage: www.elsevier.com/locate/talanta

Highly-sensitive cholesterol biosensor based on well-crystallized flower-shaped ZnO nanostructures

Ahmad Umar^{a,b,*}, M.M. Rahman^b, A. Al-Hajry^c, Y.-B. Hahn^{b,*}

^a Department of Chemistry, Faculty of Science, Najran University, P.O. Box 1988, Najran 11001, Kingdom of Saudi Arabia

^b School of Semiconductor and Chemical Engineering, BK21 Centre for Future Energy Materials and Devices, Nanomaterials Research Processing Centre, Chonbuk National University, 664-14, 6 Duckjin Dong, 1 Ga Jeonju, Choella-Bukto, Jeonju 561-756, South Korea

^c Department of Physics, Faculty of Science, Najran University, P.O. Box 1988, Najran 11001, Kingdom of Saudi Arabia

ARTICLE INFO

Article history:

Received 10 October 2008

Received in revised form 7 November 2008

Accepted 10 November 2008

Available online 25 November 2008

PACS:

62.23.Hj

82.45.Yz

87.85.Rs

81.05.Dz

81.07.-b

81.10.Bk

Keywords:

ZnO nanostructures

Flower-shaped nanostructures

Cholesterol oxidase

Cholesterol biosensor

ABSTRACT

This paper reports the fabrication of highly-sensitive cholesterol biosensor based on cholesterol oxidase (ChOx) immobilization on well-crystallized flower-shaped ZnO structures composed of perfectly hexagonal-shaped ZnO nanorods grown by low-temperature simple solution process. The fabricated cholesterol biosensors reported a very high and reproducible sensitivity of $61.7 \mu\text{A} \mu\text{M}^{-1} \text{cm}^{-2}$ with a response time less than 5 s and detection limit (based on S/N ratio) of $0.012 \mu\text{M}$. The biosensor exhibited a linear dynamic range from 1.0 – $15.0 \mu\text{M}$ and correlation coefficient of $R = 0.9979$. A lower value of apparent Michaelis–Menten constant (K_m^{app}), of 2.57 mM , exhibited a high affinity between the cholesterol and ChOx immobilized on flower-shaped ZnO structures. Moreover, the effect of pH on ChOx activity on the ZnO modified electrode has also been studied in the range of 5.0 – 9.0 which exhibited a best enzymatic activity at the pH range of 6.8 – 7.6 . To the best of our knowledge, this is the first report in which such a very high-sensitivity and low detection limit has been achieved for the cholesterol biosensor by using ZnO nanostructures modified electrodes.

© 2008 Elsevier B.V. All rights reserved.

1. Introduction

The determination of cholesterol is of vital importance since high serum cholesterol level is related to various clinical disorders, such as heart disease, coronary artery disease, arteriosclerosis, hypertension, cerebral thrombosis, and etc. [1]. In addition to this, the cholesterol and its fatty acids are also important constituents of nerve and brain cells. Hence, the development of reliable and high sensitive method for the active and fast determination of cholesterol is an active research now days. Among various determination methods, the biosensors are receiving a considerable attention due to their selectivity, fast response, reproducibility, and stability. Among various kinds of biosensors, the electrochemical biosensors which are based on the proper immobilization of enzyme on suitable matrixes offers a portable, cheap, and rapid method for the determination of various biological molecules [2–4]. Recently sci-

entists are inclined to use biocompatible nanomaterials as suitable matrixes for the enzyme immobilizations for the effective detection of various biomolecules [2–10]. Among various nanomaterials, the nanomaterials of ZnO are one of the most promising matrixes which can be use for the immobilization of various enzymes due to its numerous exotic properties such as high specific surface area, optical transparency, bio-compatibility, non-toxicity, chemical and photochemical stability, ease of fabrication, electrochemical activities, and so on [11–13]. Moreover, due to the bio-mimetic and high-electron communication features, the nanostructures of ZnO exhibiting a great potential for the fabrication of efficient chemical and biosensors [14–24]. It is observed that the high isoelectric point (IEP) of ZnO is suitable for the low IEP proteins or enzymes. Therefore, ZnO with a high IEP (~ 9.5) should be suitable for the adsorption of the low IEP enzyme (for instance ChOx IEP = ~ 4.9). Furthermore, the ZnO-modified electrode retained the enzyme bioactivity and could enhance the electron transfer between the enzyme and the electrode. Even though having various properties but there are only two reports in the literature in which ZnO nanomaterials are used as supporting matrixes to immobilize the ChOx enzymes for the effective detection of cholesterol [8,9]. Khan et al. developed a cholesterol biosensor based on ZnO nanoparticles-chitosan

* Corresponding authors. Fax: +82 63 270 2306.

E-mail addresses: ahmadumaresn@gmail.com (A. Umar), ybhahn@chonbuk.ac.kr (Y.-B. Hahn).

composite films and got the linear range of 5–300 mg dl⁻¹, detection limit of 5 mg dl⁻¹, and sensitivity of 1.41×10^{-4} A mg dl⁻¹ [8]. Singh et al. also fabricated the cholesterol biosensor based on rf-sputtered ZnO nanoporous thin films and got the linear range of 25–400 mg dl⁻¹ and response time 15 s [9]. The lower sensitivity and higher detection limit of previously fabricated ZnO nanostructures based cholesterol biosensor has been demonstrated in the literature, hence more works are needed to obtain the higher-sensitivity and lower-detection limit of the ZnO nanostructures based cholesterol biosensors.

In this paper, we are reporting an ultra-sensitive cholesterol biosensor based on flower-shaped ZnO structures composed of hexagonal-shaped ZnO nanorods. The fabricated sensor showed a very-high and reproducible sensitivity of 61.7 μ A mM⁻¹ cm⁻² with the detection limit of 0.012 μ M. Moreover, to the best of our knowledge, this is the first time such a very high-sensitivity and low-detection limit has been achieved for cholesterol biosensors by using ZnO nanostructured modified electrodes.

2. Experimental details

The entire chemicals were used as received without further purification. In a typical reaction process, 0.1 M zinc nitrate solution, made in 50.0 ml deionized water was mixed with the 0.1 M aqueous solution of hexamethylenetetramine (HMTA) (50.0 ml) under stirring at room-temperature. The resultant mixture was stirred continuously for 20 min at room temperature to mix well. Few drops of 1.0 M NaOH solution was added to adjust the pH 10.0 of the solution. The obtained solution was then heated and refluxed with continuous stirring at 100.0 °C for 9 h in necked round bottom flask. During refluxing, temperature of the solution was controlled by inserting manually adjustable thermocouple in the refluxing pot through one of its neck. White precipitates were obtained after completing the reaction which were filtered off, washed thoroughly with deionized water and ethanol, and dried at room temperature.

To fabricate the cholesterol biosensors, the as-synthesized flower-shaped ZnO structures composed of hexagonal-shaped ZnO nanorods were coated onto the surface of a gold (Au) electrode with the area of 3.0 mm². Prior to the modification, the gold electrode was polished with the 0.05 μ m alumina slurry and then sonicated in de-ionized water. The surfaces of flower-shaped ZnO structures were immobilized in a solution of ChOx (1.0 mg/mL), prepared in phosphate buffer (PBS, pH ~7.4) 150.0 mM (0.9% NaCl) for 24 h. ChOx was immobilized onto the flower-shaped ZnO structures by physical adsorption technique. The modified electrode was kept overnight for ChOx immobilization and subsequently washed with buffer solution, and dried in nitrogen environment. After drying the modified ChOx/ZnO/Au electrode, a 10 μ l Nafion solution was dropped onto the electrode and dried for 24 h at 4.0 °C to form a net-like film on the modified electrode. This step is important for the tight attachment of ZnO flowers and ChOx on the surfaces of the modified electrodes. When, not in use, the ZnO modified gold electrodes (i.e., Nafion/ChOx/ZnO/Au electrodes) were stored in PBS at 4.0 °C. The electrochemical experiments were carried out at room-temperature using an electrochemical analyzer with a conventional three-electrode configuration: a working electrode (ZnO-modified Au electrode), a Pt wire as a counter electrode and Ag/AgCl (sat. KCl) as a reference electrode.

3. Results and discussion

The general morphologies of the as-grown ZnO structures were characterized by FESEM and shown in Fig. 1 (a)–(c). From the low-magnification FESEM, it is confirmed that the grown structures are flower-shaped composed of perfectly hexagonal shaped ZnO nanorods and synthesized in a high-density with uniform

morphologies (figures (a) and (b)). It was observed from the high-resolution FESEM images that the typical lengths and diameters of the perfectly hexagonal nanorods are 300 ± 50 nm and 3 ± 1 μ m, respectively. Moreover, it is seen that all the nanorods are joined together through their bases in such a special manner that they made a beautiful-flower-shaped morphologies. The full array of one flower-shaped structure is in the range of 3–4 μ m. Inset of Fig. 1 (c) exhibits the exact morphology of the as-synthesized hexagonal-shaped ZnO nanorod grown in the flower-shaped structures. From the image, it is clear that the nanorods are formed with the six crystallographic planes where all the planes are connected each other with the internal angles of $\sim 60^\circ$. Moreover, the as-grown nanorods containing the (0001) top facets enclosed with six equivalents of $\{01\bar{1}0\}$ crystal planes. The exact hexagonal surfaces with facets confirmed the epitaxial growth and therefore the single crystalline nature of the as-grown nanorods. The crystallinity and crystal phases of the deposited ZnO nanorods were observed by the X-ray diffraction (XRD) patterns and shows in Fig. 1 (d). All of the indexed peaks in the obtained pattern are well-matched with that of bulk ZnO which confirms that the synthesized products are single crystalline and possesses a wurtzite hexagonal structures. No other peak related to impurities was detected in the pattern within the detection limit of the X-ray diffraction further confirms that the obtained products are pure ZnO. Further structural characterization of the as-grown hexagonal-shaped ZnO nanorods grown in flower-shaped structures was done by the transmission electron microscopy (TEM) and shown in Fig. 2 (a) and (b). The low-magnification TEM observation shows the exact morphology of the hexagonal-shaped ZnO nanorods assembled in flower-like structures as was seen in FESEM and reveals the full consistency in terms of shape and dimension (Fig. 2 (a)). The typical diameter of the observed nanorod is about 250 nm which possessing a very clean and smooth surfaces with the uniform diameter passim to their lengths. Fig. 2 (b) shows the high-resolution TEM (HRTEM) image which confirm that the as-grown structure is single crystalline with the lattice spacing of 0.52 nm corresponds to the *d*-spacing of [0001] crystal planes of the wurtzite hexagonal ZnO. The corresponding SAED pattern, projected along the $[2\bar{1}\bar{1}0]$ zone axis, is also consistent with the HRTEM observation and confirms that the nanorods are single crystalline with the wurtzite hexagonal phase, and preferentially grown along [0001] direction (inset 2 (b)). The composition and quality of the synthesized nanostructures was examined by FTIR in the range of 400–4000 cm⁻¹ and shown in Fig. 2 (c). A strong absorption band at 440 cm⁻¹ was observed which was related with the ZnO [25]. Two bands at ~ 3415 and ~ 1632 cm⁻¹ are correspond to the O–H stretching and bending modes of vibrations, respectively. Moreover, two very small peaks at ~ 1380 and 879 cm⁻¹ are probably due to nitrate (NO₃⁻) group as it seems that nitrate is not completely removed during the washing process [26]. Fig. 2 (d) exhibits the UV–vis. absorption spectrum, measured at room-temperature of the as-synthesized flower-shaped ZnO structures. A broad band was observed in the spectrum at 375 cm⁻¹ which is a characteristic band for the wurtzite hexagonal pure ZnO [26]. No other peak was observed in the spectrum confirms that the synthesized products are ZnO only.

A schematic of the modification of gold electrode with flower-shaped ZnO structures composed of hexagonal-shaped nanorods, ChOx and Nafion for efficient detection of cholesterol is shown in Fig. 3 (a). Fig. 3 (b) exhibits the cyclic voltammetric (CV) sweep curve for the ZnO-modified gold electrode (Nafion/ChOx/ZnO/Au) without and with 1.0 mM cholesterol in 0.1 M PBS buffer at pH 7.4 in the range of +0.3 to +0.75 V at scan rate of 100 mV/s. No redox peak was observed from the modified electrode in the absence of cholesterol however reversibly a pair of well-defined redox peaks, at +0.3 V (ox.) and +0.1 V (red.), appear from the modified electrode in presence of 1 mM cholesterol which clearly

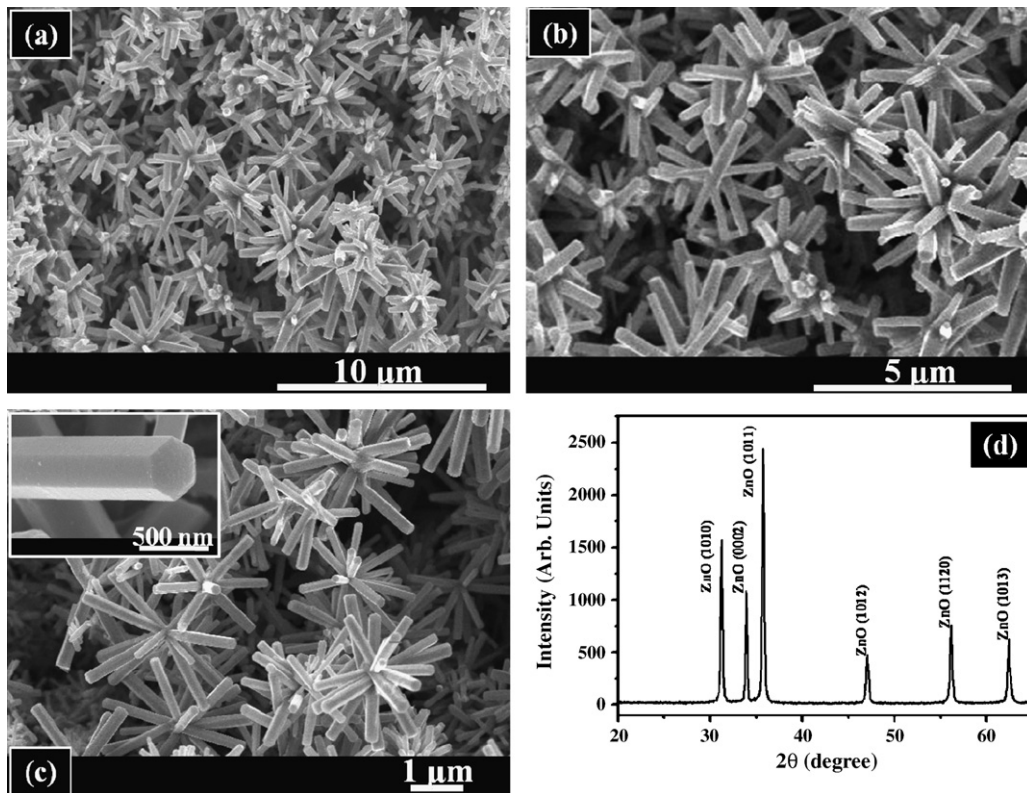


Fig. 1. (a–c) Typical FESEM images and (d) X-ray diffraction pattern of the as-grown flower-shaped ZnO structures composed of perfectly hexagonal-shaped ZnO nanorods.

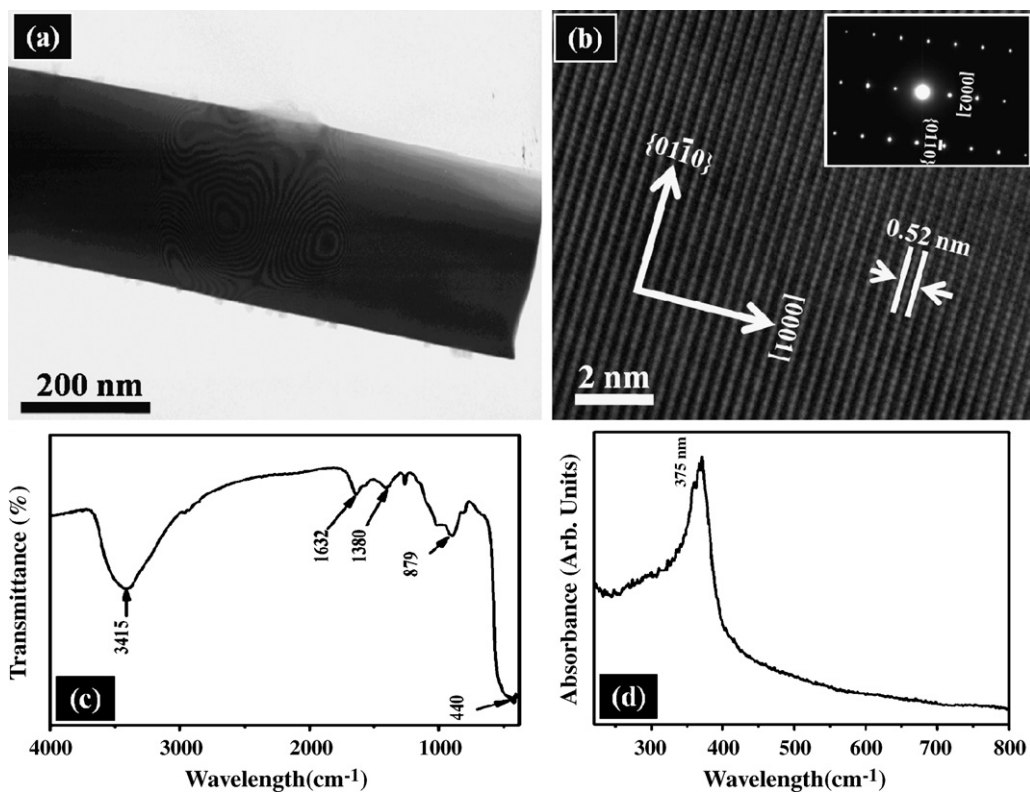


Fig. 2. Typical (a) low-magnification and (b) high-resolution and corresponding SAED pattern (inset); (c) FTIR spectrum and (d) UV-vis spectrum of the as-synthesized flower-shaped ZnO structures composed of perfectly hexagonal-shaped ZnO nanorods.

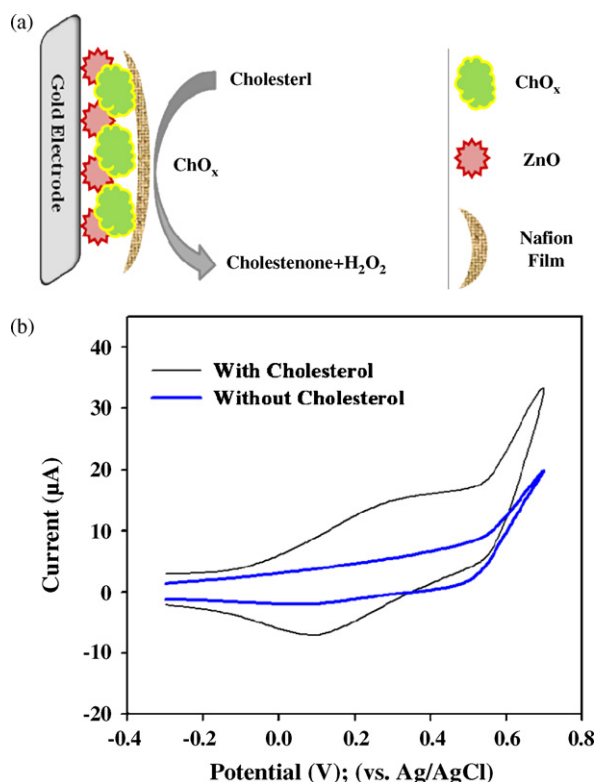


Fig. 3. (a) Schematic of the modification of gold electrode with flower-shaped ZnO structures composed of hexagonal-shaped ZnO nanorods, ChOx and Nafion for efficient detection of cholesterol; (b) cyclic voltammetric sweep curve for the Nafion/ChOx/ZnO/Au electrode without cholesterol and with 1.0 mM cholesterol in 0.1 M PBS buffer (pH 7.4) in the range of -0.3 to $+0.75$ V at scan rate of 100 mV/s.

confirms an electrochemical response from the ZnO-modified electrode in presence of cholesterol. An increase in current from -0.15 to $+0.72$ V has also been observed from the CV curve of Nafion/ChOx/ZnO/Au electrode with cholesterol in PBS compared to without cholesterol in PBS. The origination of a well-defined redox peaks from the CV curve of Nafion/ChOx/ZnO/Au electrode in PBS with 1.0 mM cholesterol are due to the H₂O₂ generation during the oxidation of cholesterol by ChOx. In addition to this, because of high surface area of flower-shaped ZnO structures composed of hexagonal-shaped nanorods, the ChOx attached to the surfaces of ZnO structures facilitates the fast and direct electron transfer

between the active sites of immobilized ChOx and electrode surface which leads to a sharper and well-defined peak. Therefore, cholesterol is efficiently detected with the Nafion/ChOx/ZnO/Au electrodes. The fast and direct electron transfer also improves the sensitivity of the fabricated biosensors. According to the previous report [9], the electrochemical reaction for the detection of cholesterol in presence of cholesterol oxidase is proposed to be as: $\text{Cholesterol} + \text{O}_2 \xrightarrow{\text{ChOx}} \text{cholestenone} + \text{H}_2\text{O}_2$ (Fig. 3 (a)).

Detailed electrochemical response experiments have been carried out on the modified Nafion/ChOx/ZnO/Au electrodes with the addition of different concentrations of cholesterol ranging from 0.1 to 25 μM in 0.1 M PBS buffer (pH 7.4) at scan rate of 100 mV/s. Fig. 4 (a) exhibits the typical CV responses of the ZnO modified electrode at different concentrations of cholesterols. It is clearly seen from the CV curves that as the concentrations of the cholesterol increases, the oxidation current also increases. The magnitude of the oxidation peak appeared at about $+0.3$ V (due to the oxidation of H₂O₂) increases due to the rising the concentration of cholesterol which is owing to the increased concentration of H₂O₂ during the enzymatic reactions. Fig. 4 (b) shows the relation between the response current and cholesterol concentration for the fabricated biosensor. It is clearly seen from the graph that the response current increases as the concentration of cholesterol increases and saturated at high concentration of cholesterol which suggests the saturation of active sites of the enzymes at those cholesterol levels. The response time for the fabricated electrode was very fast, i.e. less than 5 s, which exhibit a high electron communication feature of the used ZnO. Under optimized conditions, the steady-state current showed a linear dynamic range of 1.0–15.0 μM (Fig. 4(b)). The correlation coefficient (R) was estimated to be $R = 0.99798$ and the sensitivity was found to be $61.7 \mu\text{A} \mu\text{M}^{-1} \text{cm}^{-2}$ from the fabricated biosensor. To the best of our knowledge, this is the first time such a very high-sensitivity has been achieved for cholesterol biosensors by using ZnO nanostructures modified electrodes. The sensitivity is remarkably higher than other previously reported cholesterol biosensors based on tetraethylorthosilicate [5], polypyrrole films [6], nanoporous CeO₂ films [7], ZnO nanoparticles +chitosan composite [8], and ZnO nanoporous thin films [9], etc. Based on the signal-to-noise ratio ($S/N=3$), the detection limit of the fabricated cholesterol biosensor was estimated to be 0.012 μM which is much lower than previously reported cholesterol biosensor [5–9]. The obtained such a high-sensitivity and detection limit for the fabricated cholesterol biosensor was due to the special morphologies of the used flower-shaped ZnO structures. The used flower-shaped ZnO structures, containing hexagonal-shaped

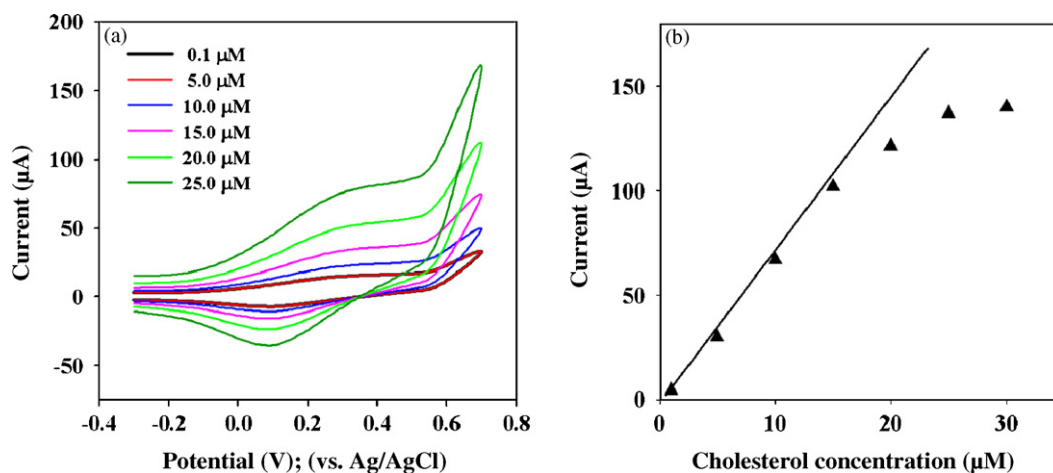


Fig. 4. (a) Electrochemical response of the Nafion/ChOx/ZnO/Au electrode at different concentrations of cholesterol i.e. 0.1, 5.0, 10.0, 15.0, 20.0, and 25.0 μM, into 0.1 M PBS buffer solution (pH 7.4); (b) calibration curve for cholesterol using modified Nafion/ChOx/ZnO/Au electrode.

Table 1
Comparison of the responses of some cholesterol biosensors constructed based on different modified electrode materials.

Electrode materials	Sensitivity ($\mu\text{A } \mu\text{M cm}^{-2}$)	Detection limit (μM)	Apparent Michaelis–Menten constant (K_m^{app}) (mM)	Linear range (μM)	Response time (s)	Reference
Tetraethylorthosilicate	–	0.500	21.2	$2.0\text{--}10.0 \times 10^3$	50	[5]
Polypyrrole films	15.0	–	9.8	$1.0\text{--}8.0 \times 10^3$	–	[6]
Nanoporous CeO_2 film	5.98	–	2.06	$1.3\text{--}10.35 \times 10^6$	15	[7]
ZnO nanoparticles +chitosan composite	14.1	0.125×10^3	0.223	$0.125\text{--}7.76 \times 10^6$	15	[8]
ZnO nanoporous thin films	–	–	2.1	$0.65\text{--}10.35 \times 10^6$	15	[9]
Flower-shaped ZnO structures composed of hexagonal-shaped nanorods	61.7	0.012	2.57	1.0–15.0	5	Current work

nanorods which were attached in three dimensions, exhibited large active surface area. Moreover, it is believed that the active surface area is directly proportional to the sensitivity and detection limit of the fabricated sensors. Hence, due to the large surface area of flower-shaped ZnO structure, large numbers of enzyme biomolecules were immobilized on the surfaces of the used ZnO structure; therefore, the ChOx attached to the surfaces of ZnO structures facilitates the fast and direct electron transfer between the active sites of immobilized ChOx and electrode surface resulting the increase in sensitivity and lowering the detection limit of the fabricated biosensor.

The apparent Michaelis–Menten constant (K_m^{app}) which gives an indication of the enzyme–substrate kinetics for the biosensor can be calculated from the electrochemical version of the Lineweaver–Burk equation $1/i = (K_m^{\text{app}}/i_{\text{max}})(1/C) + (1/i_{\text{max}})$, where i is the current, i_{max} is the maximum current measured under saturated substrate conditions, and C is the cholesterol concentration. The K_m^{app} value of the cholesterol sensor was determined by the analysis of the slope and intercept for the plot of the reciprocals of steady-state current versus cholesterol concentrations, i.e. the Lineweaver–Burk plot of $1/i$ vs. $1/C$ (Fig. 5). According to the Lineweaver–Burk plot, the K_m^{app} is calculated to be 2.57 mM. The lower K_m^{app} value means that the immobilized ChOx passes higher affinity to cholesterol. The observed K_m^{app} value for the fabricated ZnO based cholesterol biosensor is smaller than other previously reported cholesterol biosensors [5,6,10].

To check the effect of pH on the fabricated biosensor was investigated in the pH range of 5.0–9.0 at a fixed cholesterol concentration of 1.0 mM and applied potential in the range of -0.3 to $+0.75$ V at scan rate of 100 mV/s and shown in Fig. 6. It was observed that the

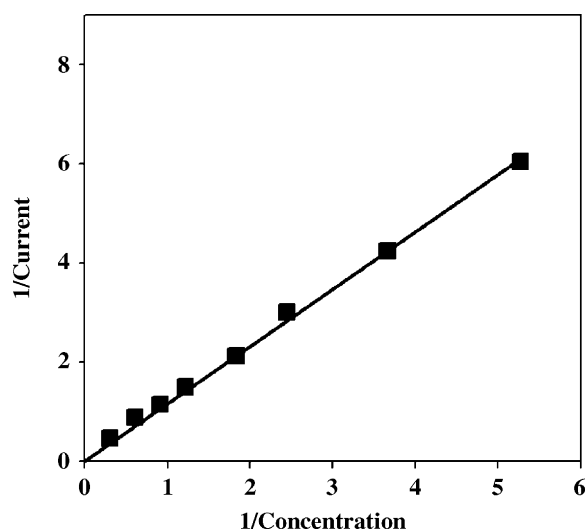


Fig. 5. The plot of $1/\text{current}$ vs. $1/\text{concentration}$ (Michaelis–Menton plot) exhibiting a linear relationship with the steady state current and cholesterol concentration.

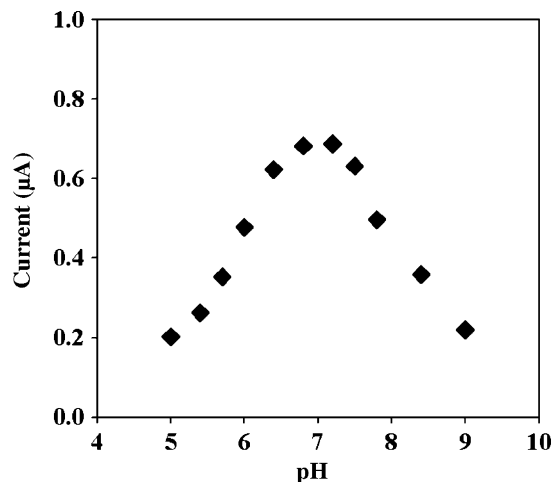


Fig. 6. The effects of pH (5.0–9.0) on the current response of the fabricated cholesterol biosensor based on the modified Nafion/ChOx/ZnO/Au electrode in 0.1 M PBS buffer (pH 7.4) in the range of -0.3 to $+0.75$ V at scan rate of 100 mV/s.

optimum pH range for the ZnO modified electrode is in the range 6.8–7.6. The rise and fall in the pH responses from the modified electrode is due to an effect of pH on the affinity of enzymes for substrate and higher stability of the enzyme in immobilized state. It is assumed that the increasing the hydrogen ion concentration ($\text{pH} < 7$) increases the successful competition of hydrogen ions for any cationic binding sites on the enzyme which results lowering the enzyme activity. Similarly, decreasing the hydrogen ions concentrations ($\text{pH} > 7.0$) means increasing the hydroxyl ions which may leads the conversion of hydroxides and can hinder the enzyme activity causes the reduction in the sensitivity of the biosensor. In this paper, the optimized pH value throughout the experiments was kept at 7.4, due to its compatibility with the human physiological condition.

For comparing, the characteristics and performances of the fabricated biosensor is compared with the previously reported cholesterol biosensors based on the utilization of various materials as the working electrode (Table 1) and it was confirmed that the presented cholesterol biosensor exhibited an excellent performance.

The fabricated biosensors exhibited very good stability and reproducibility. To check the stability of the fabricated biosensor, the experiments were conducted over a long storage period to investigate the storage stability. By repeated experiments (every 2 days) from the stored modified electrodes, it was found that the fabricated biosensors did not show any significant decrease in the sensitivity for more than 32 days, while storing in an appropriate form when not in use (at 4.0°C). It was observed that the sensitivity retained $\sim 83.7\%$ of initial sensitivity up to 32 days which gradually decreases might be due to the loss of the catalytic activity. The above results clearly suggested that the fabricated biosensor can be used for more than 1 month without any significant loss in sensitivity.

4. Conclusions

In summary, a highly-sensitive cholesterol biosensor based on ChOx immobilization on well-crystallized flower-shaped ZnO structures composed of perfectly hexagonal-shaped ZnO nanorods have been fabricated which exhibited a very high and reproducible sensitivity of $61.7 \mu\text{A} \mu\text{M}^{-1} \text{cm}^{-2}$ with a response time less than 5 s and detection limit (based on S/N ratio) of $0.012 \mu\text{M}$. The fabricated biosensor exhibited a lower value of apparent Michaelis–Menten constant (K_m^{app}), of 2.57 mM which presents a high affinity between the cholesterol and ChOx immobilized on flower-shaped ZnO structures. Importantly, to the best of our knowledge, this is the first report in which such a very high-sensitivity and low-detection limit has been achieved for the cholesterol biosensor by using ZnO nanostructures modified electrodes.

Acknowledgements

This work was partially supported by the Korea Research Foundation grant (KRF-2005-005-J07502) and by the Korea Science and Engineering Foundation grant (R01-2006-000-11306-0) funded by the Korean Government (MEST).

References

- [1] M. Nauck, W. Marz, H. Wieland, *Clin. Chem.* 46 (2000) 436.
- [2] A. Umar, M.M. Rahman, S.H. Kim, Y.B. Hahn, *Chem. Commun.* (2008) 166.
- [3] A. Umar, M.M. Rahman, S.H. Kim, Y.B. Hahn, *J. Nanosci. Nanotech.* 8 (2008) 3216.
- [4] A. Umar, M.M. Rahman, Y.B. Hahn, *Talanta* 77 (2009) 1376.
- [5] A. Kumar, R. Malhotra, B.D. Malhotra, S.K. Grover, *Anal. Chim. Acta* 414 (2000) 43.
- [6] S. Singh, A. Chaubey, B.D. Malhotra, *Anal. Chim. Acta* 502 (2004) 229.
- [7] A. Ansari, A. Kaushik, P. Solanki, B. Malhotra, *Electrochem. Commun.* 10 (2008) 1246.
- [8] R. Khan, A. Kaushik, P. Solanki, A. Ansari, M. Pandey, B. Malhotra, *Anal. Chim. Acta* 616 (2008) 207.
- [9] S. Singh, S. Arya, P. Pandey, B. Malhotra, S. Saha, K. Sreenivas, V. Gupta, *App. Phys. Lett.* 91 (2007) 63901.
- [10] C. Bongiovanni, T. Ferri, A. Poscia, M. Viralli, R. Santucci, A. Desideri, *Bioelectrochemistry* 54 (2001) 17.
- [11] A. Umar, Y.B. Hahn, *Appl. Phys. Lett.* 88 (2006) 173120.
- [12] A. Umar, B. Karunakaran, S.H. Kim, E.K. Suh, Y.B. Hahn, *Inorg. Chem.* 47 (2008) 4088.
- [13] A. Umar, Y.B. Hahn, *Cryst. Growth Des.* 8 (2008) 2741.
- [14] Z.R.R. Tian, J.A. Voigt, J. Liu, B. McKenzie, M. McDermott, *J. Am. Chem. Soc.* 124 (2002) 12954.
- [15] G. Sberveglieri, S. Groppelli, P. Nelli, A. Tintinelli, G. Giunta, *Sens. Actuators B* 25 (1995) 588.
- [16] J.A. Rodriguez, T. Jirsak, J. Dvorak, S. Sambasivan, D. Fischer, *J. Phys. Chem. B* 104 (2000) 319.
- [17] F. Zhang, X. Wang, S. Ai, Z. Sun, Q. Wan, Z. Zhu, Y. Xian, L. Jin, K. Yamamoto, *Anal. Chim. Acta* 519 (2004) 155.
- [18] Y. Liu, Y. Yang, H. Yang, Z. Liu, G. Shen, R. Yu, *J. Inorg. Biochem.* 99 (2005) 2046.
- [19] Y. Li, Z. Liu, Y. Liu, Y. Yang, G. Shen, R. Yu, *Anal. Biochem.* 349 (2006) 33.
- [20] Z.W. Zhao, X.J. Chen, B.K. Tay, J.S. Chen, Z.J. Han, K.A. Khor, *Biosens. Bioelect.* 23 (2007) 135.
- [21] C.D. Corso, A. Dickherber, W.D. Hunt, *Biosens. Bioelect.* 24 (2008) 811.
- [22] Z. Deng, Y. Tian, X. Yin, Q. Rui, H. Liu, Y. Luo, *Electrochem. Commun.* 10 (2008) 818.
- [23] L. Chen, B. Gu, G. Zhu, Y. Wu, S. Liu, C. Xu, *J. Electroanal. Chem.* 617 (2008) 7.
- [24] X. Lu, H. Zhang, Y. Ni, Q. Zhang, J. Chen, *Biosens. Bioelect.* 24 (2008) 93.
- [25] L. Wu, Y. Wu, Lu Wei, *Physica* 28 (2005) 76.
- [26] Y.H. Ni, X.W. Wei, J.M. Hong, Y. Ye, *Mater. Sci. Eng. B* 121 (2005) 42.